Streamflow responses to past and projected future changes in climate at the Hubbard Brook Experimental Forest, New Hampshire, United States

John L. Campbell,[1] Charles T. Driscoll,[2] Afshin Pourmokhtarian,[2] and Katharine Hayhoe[3]

Received 19 April 2010; revised 7 September 2010; accepted 25 October 2010; published 11 February 2011.

[1] Climate change has the potential to alter streamflow regimes, having ecological, economic, and societal implications. In the northeastern United States, it is unclear how climate change may affect surface water supply, which is of critical importance in this densely populated region. The objective of this study was to evaluate the impact of climate change on the timing and quantity of streamflow at small watersheds at the Hubbard Brook Experimental Forest in New Hampshire. The site is ideal for this analysis because of the availability of long-term hydroclimatological records for analyzing past trends and ample data to parameterize and test hydrological models used to predict future trends. In this study, future streamflow projections were developed with the forest watershed model PnET-BGC, driven by climate change scenarios from statistically downscaled outputs of atmospheric-ocean general circulation models. Results indicated that earlier snowmelt and the diminishing snowpack is advancing the timing and reducing the magnitude of peak discharge associated with snowmelt. Past increases in precipitation have caused annual water yield to increase significantly, a trend that is expected to continue under future climate change. Significant declines in evapotranspiration have been observed over the long-term record, although the cause has not been identified. In the future, evapotranspiration is expected to increase in response to a warmer and wetter environment. These increases in evapotranspiration largely offset increases in precipitation, resulting in relatively little change in streamflow. Future work should aim to decrease uncertainty in the climate projections, particularly for precipitation, obtain a better understanding of the effect of CO_2 on vegetation, determine if climate-induced changes in tree species composition will influence discharge, and assess the impacts of changing hydrology on downstream water supplies.

Citation: Campbell, J. L., C. T. Driscoll, A. Pourmokhtarian, and K. Hayhoe (2011), Streamflow responses to past and projected future changes in climate at the Hubbard Brook Experimental Forest, New Hampshire, United States, *Water Resour. Res., 47*, W02514, doi:10.1029/2010WR009438.

1. Introduction

[2] Climate change is emerging as the single most important environmental issue of the 21st century. Global air temperatures have increased by 0.74°C over the last 100 years [*Intergovernmental Panel on Climate Change* (*IPCC*), 2007]. Precipitation is also changing in volume, intensity, and form (e.g., rain and snow) throughout many regions of the world [*Dore*, 2005; *IPCC*, 2007]. These shifts in climate ultimately affect the quantity and seasonal distribution of streamflow, having important implications for global water supplies. In some regions of the world, streamflow is increasing, whereas decreases are occurring in other regions [*Milly et al.*, 2005]. The direction and extent of change in streamflow is dictated by the relative balance between precipitation and the processes that govern evapotranspiration (ET), such as air temperature, air humidity, solar radiation, wind speed, atmospheric CO_2 concentration, and vegetation characteristics.

[3] In the United States, concerns about changes in streamflow regimes have primarily focused on western regions, where runoff is generated by snowmelt. Reductions in winter snowpack in the mountainous West have altered streamflow timing [*Cayan et al.*, 2001; *Dettinger and Cayan*, 1995; *Hidalgo et al.*, 2009; *Regonda et al.*, 2005; *Stewart et al.*, 2005], which may limit future availability [*Barnett et al.*, 2005; *Christensen et al.*, 2004], contributing to an ever-increasing demand for water. Climate-induced changes in streamflow in the northeastern United States have received much less attention, despite observed and projected future snowpack declines [*Burakowski et al.*, 2008; *Campbell et al.*, 2010; *Hodgkins and Dudley*, 2006] and decreases in snowfall [*Burakowski et al.*, 2008; *Huntington et al.*, 2004]. While snowmelt is not the dominant source of streamflow in the Northeast as it is in the West, it

[1]Northern Research Station, U.S. Forest Service, Durham, New Hampshire, USA.
[2]Department of Civil and Environmental Engineering, Syracuse University, Syracuse, New York, USA.
[3]Department of Geosciences, Texas Tech University, Lubbock, Texas, USA.

0043-1397/11/2010WR009438

does contribute to groundwater recharge, potentially influencing water supply. Consequently, even though water is relatively abundant in the Northeast, changes in the snowpack and streamflow could affect stream ecosystem services in the region, such as drinking water, irrigation, recreation, wastewater assimilation, and power generation.

[4] Evidence of climate change in the northeastern United States is well documented [*Hayhoe et al.*, 2007; *Huntington et al.*, 2009; *Keim et al.*, 2003; *Trombulak and Wolfson*, 2004]. Analyses of long-term air temperature data show a warming trend of 0.8°C ± 0.1°C over the 20th century [*Hayhoe et al.*, 2007]. Precipitation is more variable but has increased by an average of 95 ± 20 mm during the same time period [*Hayhoe et al.*, 2007]. The greatest increases in air temperature have occurred during winter, whereas there has been negligible change in the amount of winter precipitation [*Hayhoe et al.*, 2007] and a decline in the proportion of precipitation falling as snow [*Huntington et al.*, 2004]. These trends in climate have led to a reduction in the winter snowpack [*Burakowski et al.*, 2008; *Campbell et al.*, 2010; *Hodgkins and Dudley*, 2006], which in turn has altered streamflow dynamics. One of the most notable changes in streamflow has been an advance in the timing of spring freshet and a more uniform distribution of flow throughout the snowmelt period [*Hartley and Dingman*, 1993; *Hodgkins et al.*, 2003]. March streamflows have generally increased and May streamflows have declined [*Hodgkins and Dudley*, 2005]. However, significant changes in the duration and magnitude of base flow and the volume of annual streamflow have not been observed [*Hodgkins et al.*, 2005].

[5] Despite evidence that past trends in climate have altered streamflow timing in the Northeast, it is unclear how future streamflow will be affected by climate forcing. Climate projections for the Northeast indicate a regional warming of 2.1°C to 5.3°C and a 7%–14% increase in annual precipitation by the end of this century, depending on both the atmosphere-ocean general circulation model (AOGCM) used and greenhouse gas (GHG) emission scenario [*Hayhoe et al.*, 2007]. Previous modeling work has indicated that future climate change will result in a reduction in spring snowmelt and the potential for snowmelt-induced episodic acidification, having important implications for the supply and quality of stream water [*Davies and Vavrus*, 1991]. Empirical statistical models suggest that streamflow will be significantly lower under a warmer climate because of an increase in ET [*Huntington*, 2003]. Empirical modeling approaches provide useful insight; however, they lack predictive ability for unprecedented future conditions. As an alternative, process-based models can be used. While these models are only capable of representing processes to the extent that they are quantitatively understood, they provide a robust framework for assessing hydrologic responses to climate change. The advent of AOGCM climate downscaling techniques has made it possible to run these models with more precise climate projections for specific locations.

[6] Headwater streams can be useful for studying the influence of climate change on streamflow because they have small contributing areas with shallow soils, making them highly responsive to changes in energy, water, and chemical inputs. These low-order stream networks are the source waters for larger rivers and therefore may serve as a bellwether for climate change effects. In this study, we examined the influence of climate change on streamflow at small, gauged watersheds at the Hubbard Brook Experimental Forest (HBEF) in New Hampshire. The site is well suited for this analysis because there are long-term records of streamflow from multiple watersheds for evaluating trends as well as extensive ancillary explanatory data (e.g., temperature, precipitation, solar radiation, snowpack, and net primary productivity (NPP)). These comprehensive long-term data are also necessary for running and validating models that simulate the effect of climate change on streamflow.

[7] The major objectives of the study were to (1) determine if past changes in climate have affected the quantity and distribution of streamflow at the HBEF and (2) evaluate the effects of potential future climate regimes on streamflow. Our central hypothesis is that climate change alters the seasonal distribution and decreases the overall quantity of stream water primarily because of the loss of the seasonal snowpack and enhanced ET.

2. Methods

2.1. Study Site

[8] The HBEF (43°56′N, 71°45′W) is located in the White Mountain National Forest in central New Hampshire. The climate is cool, humid, and continental, with average monthly air temperatures ranging from −9°C in January to 18°C in July. Precipitation is distributed fairly evenly throughout the year (annual mean of 1400 mm), with one third occurring as snow. On average, the snowpack persists from late December until mid-April. Vegetation is predominantly northern hardwood (*Fagus grandifolia* Ehrh., *Acer saccharum* Marsh., and *Betula alleghaniensis* Britt.), with coniferous species (*Picea rubens* Sarg. and *Abies balsamea* (L.) Mill.) occurring at higher elevations and on steeper slopes. Spodosols are the dominant soil type; Typic Haplorthods derived from glacial basal till. They have a sandy loamy texture and are well drained and shallow, with bedrock occurring at a depth of 1–2 m.

[9] Streamflow data from four of the nine gauged watersheds at the HBEF were used in this study (Figure 1 and Table 1). This subset of watersheds was selected on the basis that they have not been experimentally manipulated and have long-term (40–51 years) records. Two of the watersheds are located on south facing slopes (W3, W6) and the other two are on north facing slopes (W7, W8). Differences in elevation and aspect between north and south facing watersheds influence watershed characteristics such as air temperature, amount and type of precipitation, snowpack development and ablation [*Bailey et al.*, 2003], and tree species composition [*Schwarz et al.*, 2003].

2.2. Field Measurements

[10] Streamflow has been recorded at the outlet of each of the study watersheds beginning as early as water year 1959 (Table 1). Continuous streamflow measurements are made using stage height recorders and either a solitary V notch weir or V notch weir in conjunction with a San Dimas flume (Table 1) [*Reinhart and Pierce*, 1964].

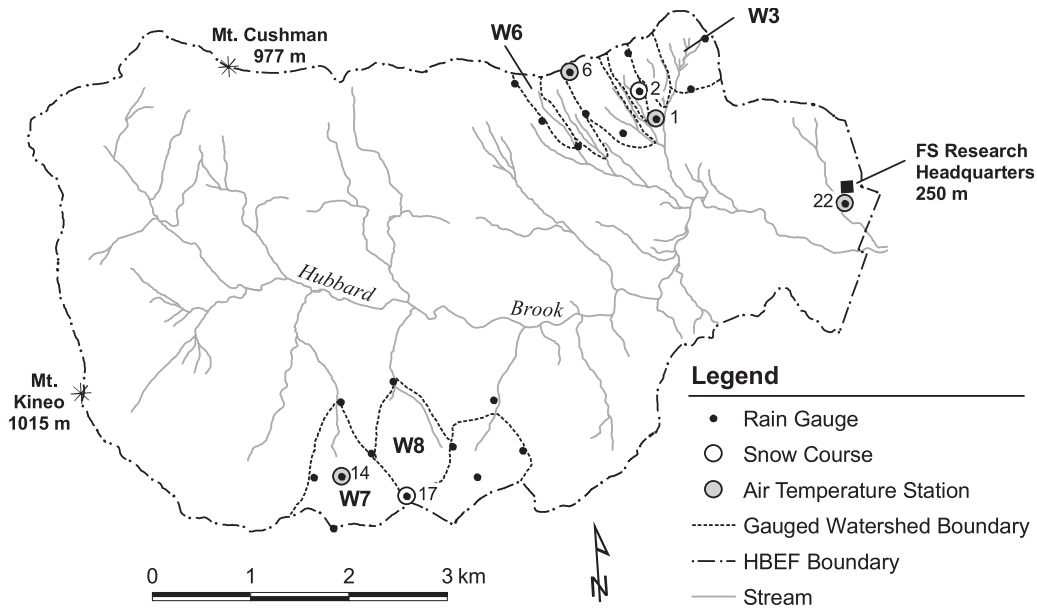

Figure 1. Map of the HBEF (43°56′N, 71°45′W) showing the watersheds used in this study (W3, W6, W7, and W8), rain gauge locations, and weather stations with long-term snow course (stations 2 and 17) and air temperature data (stations 1, 6, 14, and 22).

Streamflow is expressed in millimeters and is calculated by normalizing the instantaneous flow rates (liters per second) by watershed area and integrating over time.

[11] Precipitation is measured in clearings with a network of standard and continuous recording rain gauges. Rain gauges are distributed throughout the area of the experimental watersheds to capture variation associated with elevation and topography (Figure 1). Rainfall amounts at standard gauges are recorded weekly. Daily precipitation for a standard gauge is determined by prorating its weekly total using daily totals from the nearest continuous recording gauge [*Bailey et al.*, 2003]. Precipitation for each entire watershed is calculated as the areal weighted daily average of three to six nearby rain gauges. Annual ET (sum of evaporation and plant transpiration) was calculated as the difference between precipitation and streamflow, which is based on the assumption that changes in storage over the long-term are negligible and the underlying bedrock is reasonably watertight [*Likens and Bormann*, 1995]. While groundwater loss at some research watersheds is significant, it is thought to be minimal at Hubbard Brook because of the impermeable bedrock that underlies the watersheds [*Likens and Bormann*, 1995; *Verry*, 2003]. At three of the watersheds (W3, W6, and W8), precipitation measurements started a year after streamflow measurements, so the length of record for precipitation and, hence, ET is 1 year shorter than streamflow. Data are reported using a 1 October water year (WY, e.g., WY 2008 is from 1 October 2007 through 30 September 2008). Seasonal designations coincided with the WY and included fall (October–December), winter (January–March), spring (April–June), and summer (July–September).

[12] Other basic meteorological measurements have been collected in, or adjacent to, rain gauge clearings (Figure 1). Air temperature has been measured with hygrothermographs housed in standard shelters (Stevenson screens) since the inception of the HBEF in 1955. Air temperature records from stations 1, 6, 14, and 22 were used in this analysis because they have the longest records (52, 47, 43, and 51 years, respectively) and are representative of the range in temperature encountered at the HBEF. Solar radiation, which is required input for PnET-BGC, has been measured with a pyranometer since 1960, adjacent to rain gauge 22. Long-term snowpack data have been collected at stations 2 and 17 along "snow courses" located under the forest canopy [*Campbell et al.*, 2010]. A "snow course" consists of a transect of 10 points spaced at 2 m intervals. Each week, snow depth and snow water equivalent are measured at each point using a Mount Rose snow tube. The following week a parallel transect, 2 m from the previous one, is used.

Table 1. Characteristics of the Study Watersheds

Watershed	Initial Water Year[a]	Area (ha)	Elevation (m)	Slope (deg)	Aspect	Stream Gauge
W3	1959	42.4	527–732	12.1	S23°W	V notch
W6	1964	13.2	549–792	15.8	S32°E	V notch, flume
W7	1966	77.4	619–899	12.4	N16°W	V notch, flume
W8	1969	59.4	610–905	14.0	N12°W	V notch, flume

[a]Water Year from 1 October to 30 September.

2.3. Model Description

[13] Past and future projected streamflow was modeled using the comprehensive forest soil water model PnET-BGC. PnET-BGC is a lumped parameter watershed model that simulates energy, water, and element flows through vegetation and soil to surface waters. PnET-BGC builds on the C, N, and water balance model PnET-CN [*Aber and Federer*, 1992] to include the cycling of major elements (i.e., C, N, P, S, Ca, Mg, K, Na, Al, Cl, and Si). Both major biotic and abiotic processes are represented, including atmospheric deposition, canopy interaction, hydrology, soil organic matter dynamics, mineral weathering, and chemical reactions involving solid and solution phases. The model has been used extensively to assess the effects of land disturbance and air pollution on forest and aquatic ecosystems [*Chen and Driscoll*, 2005a, 2005b; *Gbondo-Tugbawa and Driscoll*, 2003; *Gbondo-Tugbawa et al.*, 2002] and has recently been used to evaluate climate change impacts [*Campbell et al.*, 2009]. A thorough description of the model with the processes depicted, model validation, and a detailed sensitivity analysis of parameter values is provided by *Gbondo-Tugbawa et al.* [2001].

[14] While PnET-BGC is not a traditional hydrologic model, there are compelling reasons why it can serve as an important tool for assessing climate change impacts on streamflow. Unlike traditional hydrologic models, the depiction of hydrologic dynamics in PnET-BGC is closely coupled with water use by vegetation [*Aber and Federer*, 1992]. As a result, changes in forest growth and phenology associated with climate change are manifested in water fluxes. The inclusion of interactions between nutrient cycling, terrestrial vegetation, and hydrology in PnET-BGC is essential for evaluating the effect of climate change on future streamflow and extends the work of previous climate change modeling efforts in the Northeast, which have been more limited in scope [e.g., *Davies and Vavrus*, 1991]. A recent addition to PnET-BGC is an algorithm that depicts the effect of increasing atmospheric CO_2 on photosynthesis and stomatal conductance [*Ollinger et al.*, 2008], which may have implications for streamflow [*Gedney et al.*, 2006]. While some evidence indicates that the effect of increasing atmospheric CO_2 on transpiration over the 20th century has had relatively minor effects on streamflow [*Huntington*, 2008], the inclusion of these processes in the model enables the evaluation of future effects. In the present study, we did not consider climate-induced changes in forest composition which could also influence streamflow by altering transpiration [e.g., *Swank and Douglass*, 1974]. Past studies have shown that potential suitable habitat of tree species may shift northward [*Iverson and Prasad*, 1998; *Iverson et al.*, 2008]; however, the migration of established species may take much longer [*Iverson et al.*, 2004] and is not well understood. Consequently, the effect of changes in tree species composition was not considered in this application.

[15] The hydrological component of PnET-BGC is governed by a simple water balance (Figure 2). Two water storage compartments are represented in the model: snowpack and soil. The water balance equation for the snowpack is expressed as

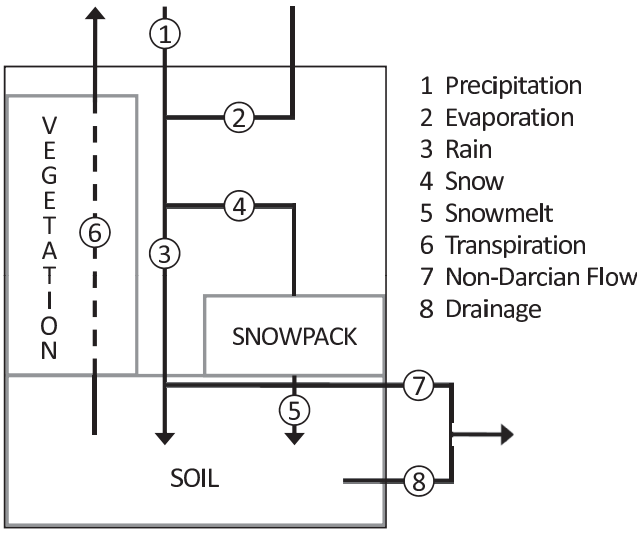

Figure 2. Hydrological compartments and processes represented in the PnET-BGC model.

$$\frac{dm^w_{snow}}{dt} = S^w_{snow} - S^w_{melt}\left(m^w_{snow}\right), \tag{1}$$

where the evolution of the snowpack state variable m^w_{snow} in time is determined by the difference between the amount of precipitation that falls as snow S^w_{snow} and snowmelt S^w_{melt} from the available water stored in the snowpack m^w_{snow}.

[16] The soil water balance equation combines the snow water component in equation (1) with other hydrological processes represented in the model:

$$\frac{dm^w_{soil}}{dt} = S^w_{prec} - S^w_{evap} - S^w_{snow} + S^w_{melt}\left(m^w_{snow}\right) - S^w_{trans}\left(v, m^w_{soil}\right) - S^w_{f\,flow} - S^w_{drain}\left(m^w_{soil}\right). \tag{2}$$

[17] A fraction of precipitation input S^w_{prec} (1 in Figure 2) is evaporated S^w_{evap} (2), and the remainder is partitioned into rain (3) or snow (4), depending on the air temperature. Snowmelt (5) is calculated using an empirical degree day approach. Transpiration S^w_{trans} (6) is dependent on climatic conditions as well as the state of the vegetation v and the availability of water in soil. Non-Darcian (macropore) fast flow $S^w_{f\,flow}$ (7) is accounted for by a constant fraction of water that bypasses the plant available soil water pool. If water stored in the soil pool for the period of the time step exceeds the soil water holding capacity, the difference is considered to be drainage S^w_{drain} (8). Further details about the hydrological aspects of PnET-BGC are provided by *Aber and Federer* [1992].

[18] In this application, PnET-BGC was run for the reference watershed (W6) on a monthly time step. Watershed 6 was selected among the other watersheds for this analysis based on the better availability of data used to run and validate the model. The model was initially run for WY 1960–2008 using measured climate data, including precipitation from W6, minimum and maximum air temperature from station 1, and photosynthetically active radiation (PAR), as

Table 2. Description and Definition of Model Performance Measures

Measure	Abbreviation	Description	Mathematical Definition[a]
Nash-Sutcliffe model efficiency	NSME	Variation in measured values accounted for by the model	$1-\frac{\sum_{i=1}^{n}(Y_i-\hat{Y}_i)^2}{\sum_{i=1}^{n}(Y_i-\bar{Y})^2}$
RMSE and observation standard deviation ratio	RSR	Ratio of the root-mean-square error and standard deviation of observed values	$\frac{\sqrt{\sum_{i=1}^{n}(Y_i-\hat{Y}_i)^2}}{\sqrt{\sum_{i=1}^{n}(Y_i-\bar{Y})^2}}$
Percent bias	PBIAS	Difference between observed and simulated values expressed as a percent	$\frac{\sum_{i=1}^{n}(Y_i-\hat{Y}_i)}{\sum_{i=1}^{n}(Y_i)}\times 100$

[a] Y is observed values, $\bar{Y}$ is the mean of observed values, $\hat{Y}$ is simulated values, and n is the number of observations.

calculated with the method of *Aber and Freuder* [2000] using solar radiation data from station 22 (Figure 1). PnET-BGC was evaluated by comparing simulated streamflow with measured streamflow at W6. Three metrics of model performance were used in accordance with the work of *Moriasi et al.* [2007]: Nash-Sutcliffe model efficiency (NSME [*Nash and Sutcliffe*, 1970]), the ratio of root-mean-square error to the standard deviation of measured data (RSR), and percent bias (PBIAS; Table 2). Values of NMSE can range from $-\infty$ to 1, with 1 being optimal. RSR can vary from the optimal value of 0, which indicates a perfect model fit, to a large positive value. The optimal value for PBIAS is 0, with positive values overestimating and negative values underestimating the observed data.

2.4. Future Scenarios

[19] In addition to running the model with past measured climate input data, future streamflow simulations (WY 2009–2099) for W6 were run using climate data from statistically downscaled AOGCM output archived in the IPCC database by the Program for Climate Model Intercomparison and Diagnosis. The AOGCMs used were the Geophysical Fluid Dynamics Laboratory Model (GFDL [*Delworth et al.*, 2006]), the Hadley Centre Coupled Model, version 3 (HadCM3 [*Pope et al.*, 2000]), and the Parallel Climate Model (PCM [*Washington et al.*, 2000]). Additionally, two future atmospheric GHG emissions scenarios (B1 and A1FI) were selected, for a total of six climate projections (three AOGCMs times two emissions scenarios). The A1FI (higher) and B1 (lower) emissions scenarios correspond to potential atmospheric CO_2 concentrations of 970 and 550 ppm, respectively, by 2100 [*Nakicenovic et al.*, 2000]. This is roughly equivalent to more than a tripling (A1FI) and doubling (B1) of atmospheric CO_2 concentrations relative to preindustrial levels.

[20] Global, coarse-resolution AOGCM outputs have been statistically downscaled for the northeastern United States to a 1/8° horizontal resolution [*Hayhoe et al.*, 2008]. An empirical statistical approach was used where probability density functions for modeled climate data were mapped onto those of gridded historical observed data. The method involves a bias correction and spatial disaggregation technique that was originally developed for adjusting AOGCM output for long-range streamflow forecasting [*Wood et al.*, 2002]. Results from this approach compare favorably to other statistical and dynamic downscaling techniques [*Hayhoe et al.*, 2008; *Wood et al.*, 2004]. Climate projections specific to the HBEF were extracted from the grid cell coinciding with the location of the study site. Since the spatial resolution of the statistically downscaled data is still coarse relative to the size of the reference watershed (13.87 versus 0.13 km^2), there is a potential for biases in the modeled climate data. To check for biases, the statistically downscaled climate data were compared to measured data for the reference period (1960–2008). Simulated monthly air temperature and PAR closely matched the measured data (Figure 3). However, precipitation for all three models was approximately 20% lower than the measured values, likely because of local affects of mountainous topography. Following *Ollinger et al.* [2008], projected precipitation amounts for the HBEF were scaled upward by 20% to account for this discrepancy. There are no seasonal trends in precipitation at the HBEF, and on a

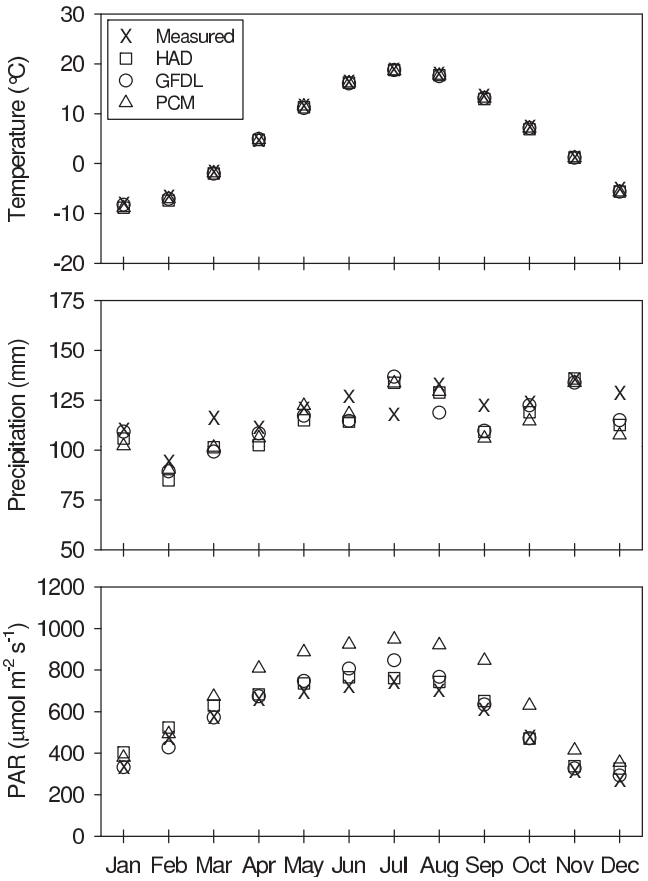

Figure 3. Comparison of mean monthly measured climate data with data statistically downscaled from three AOGCMs for the reference period (1965–2008).

monthly basis the corrected modeled values were comparable to the measured values (Figure 3).

[21] Because there is more uncertainty in how future precipitation will change compared to future air temperature [*Hayhoe et al.*, 2007], we conducted an additional set of PnET-BGC model simulations using detrended precipitation. Future precipitation for each scenario was detrended by calculating the slope for 2009–2099, as described in section 2.5 and decreasing the monthly precipitation values accordingly. PnET-BGC was then rerun using these detrended precipitation input values to evaluate the effect of future trends in precipitation on streamflow.

[22] In addition to climate input, PnET-BGC also requires wet and dry deposition values for major elements. Estimates of future atmospheric deposition were based on a "business-as-usual" deposition scenario developed for the northeastern United States using the Community Multiscale Air Quality model (http://www.epa.gov/AMD/CMAQ/). The deposition scenario used in PnET-BGC is representative of current average trends and thus assumes no change in emissions.

2.5. Statistical and Data Analyses

[23] Time series trends were evaluated using the nonparametric Mann-Kendall (MK) test that is commonly used for analyses of long-term hydrometeorological data [*Helsel and Hirsch*, 1992; *Hirsch et al.*, 1982]. One of the advantages of this test is that it is rank based, making it suitable for nonnormally distributed data, data containing outliers, and nonlinear trends. Where seasonal cycles existed (e.g., temperature, streamflow, and ET), the seasonal Kendall (SK) test for trends was used. This test is a modification of the MK test [*Helsel and Hirsch*, 1992; *Kendall*, 1938] and is designed to eliminate confounding variation associated with seasonality. The SK test calculates MK test statistics separately for each season and combines the results. Prior to this analysis, the nonparametric autocorrelation function (ACF) test was used to determine whether the data met the assumption of serial independence. When serial correlation was present, a modified SK test was used that produces adjusted p values by accounting for covariance [*Hirsch and Slack*, 1984]. Reported p values were considered significant at the $\alpha = 0.10$ level. The nonparametric Kendall-Theil robust line (KTRL) was fitted to the data to quantify change over time. The slope of the KTRL was determined with the seasonal Kendall slope estimator and is calculated as the median slope of all possible pairs in the data set [*Sen*, 1968]. The intercept was established by intersecting the slope with the median of the dependent and independent variables.

[24] Changes in streamflow timing were evaluated with center of volume dates (CVD [*Court*, 1962; *Hodgkins et al.*, 2003]) for annual (October–September), fall (October–December), and winter/spring (January–June) time periods. The fall and winter/spring periods correspond with seasonal peaks in the hydrograph. Changes in streamflow timing were also evaluated using the method of *Déry et al.* [2009], where KTRL slopes are calculated for sequent 5 day means of runoff, an approach that reveals more detailed structure of changes in streamflow timing. In this approach, the initial and final years of the record are compared using the end points of the trend line, which eliminates bias associated with evaluating the actual measured values for those years. Changes in high and low daily flows were evaluated by establishing high (90th and 75th percentiles) and low (10th and 25th percentiles) daily flow thresholds and calculating trends in the number of days that respectively exceed or fall below these thresholds.

3. Results

3.1. Past Hydroclimatological Trends

[25] Long-term air temperature and precipitation data from the HBEF indicate that the climate has changed over the period of measurement. Air temperature increased significantly ($p < 0.05$) at all weather stations by 0.017°C–0.029°C yr^{-1} (Figure 4). Increases were distributed fairly evenly among the seasons, although during fall, increases were only significant at one station ($p = 0.074$, station 22). Annual precipitation also increased at all watersheds evaluated; however, increases were only significant at W3 ($p = 0.052$), which had the longest record (Figure 4). None of the seasonal trends in precipitation were statistically significant.

[26] Snow course data from stations 2 and 17 show that the snowpack has declined significantly at the HBEF over the period of measurement (1966–2008). For months that have consistent snow cover from year to year (January, February, and March), average monthly snow water equivalent declines range from 0.16 to 0.22 cm yr^{-1} over the 43 years of measurement (Table 3). Snow water equivalent modeled with PnET-BGC also showed significant declines for the same time period, although trend line slopes for

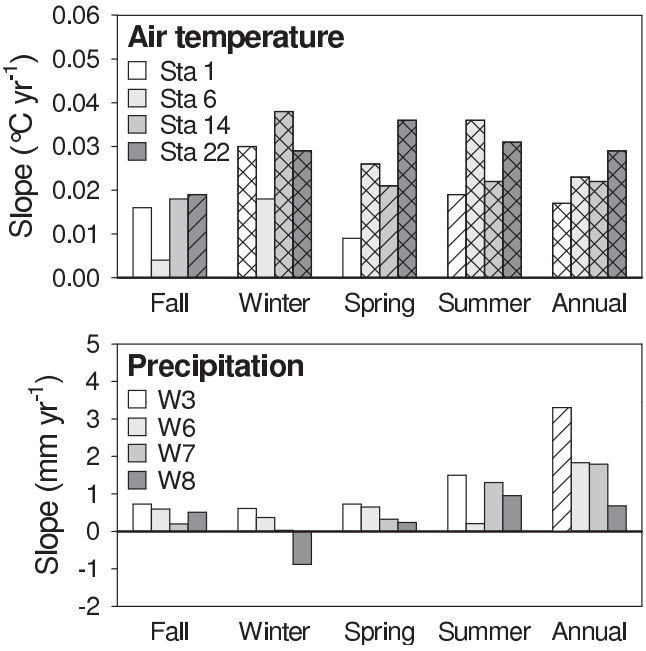

Figure 4. Seasonal and annual trends in measured air temperature (stations 1, 6, 14, and 22) and precipitation (W3, W6, W7, and W8) for all the available years of data through WY 2008. Crosshatches indicate the 0.05 level of significance, and single hatches indicate the 0.10 level of significance.

Table 3. Mean Snow Water Equivalent and Change for January, February, March, and the Average for All Three Months[a]

	Station 2 (Measured)		Station 17 (Measured)		Watershed 6 (Modeled)	
Period	Mean (cm)	Slope (p Value)	Mean (cm)	Slope (p Value)	Mean (cm)	Slope (p Value)
January	8.1	−0.20 (0.001)[c]	11.1	−0.17 (0.021)[c]	11.2	−0.08 (0.315)
February	13.1	−0.19 (0.023)[c]	17.7	−0.16 (0.077)[b]	14.4	−0.11 (0.202)
March	13.87	−0.22 (0.027)[c]	22.9	−0.22 (0.042)[c]	15.1	−0.12 (0.143)
January–March	11.7	−0.20 (0.000)[c]	17.2	−0.18 (0.000)[c]	13.5	−0.10 (0.029)[c]

[a]The Kendall-Theil robust line (KTRL) slope (cm yr^{-1}) and associated p values are shown for WY 1966–2008. Values for stations 2 and 17 are from weekly snow course measurements, and values for W6 were modeled with PnET-BGC.
[b]Significance $p < 0.10$.
[c]Significance $p < 0.05$.

each month were not as steep and were only significant for the average of all three winter months (January, February, and March). Additional snow metrics and evidence of the diminishing snowpack at the HBEF are provided by *Campbell et al.* [2010].

[27] Significant shifts in streamflow timing were also evident. The annual CVD occurred 0.19–0.45 d yr^{-1} earlier when all the years of available data were evaluated and 0.22–0.45 d yr^{-1} earlier when data from a common time period (1969–2008) were evaluated (Table 4). The winter/spring CVD also occurred earlier at most of the watersheds. Significant trends were generally more common when all of the years of data available were included as compared to when only data from a common time period (1969–2008) were evaluated. Despite shorter periods of data collection at north facing W7 and W8, trends tended to be more strongly significant at these watersheds relative to south facing W3 and W6, which had longer records. There were no significant trends in the fall CVD at any of the watersheds. At all watersheds, comparisons between the initial WY and WY 2008, as determined by the endpoints of the KTRL, show a shift toward an earlier and more muted spring freshet (Figure 5). The overall trend changes from a positive slope in early spring to a negative slope later in the snowmelt period.

[28] The trend in the number of low- and high-flow days per year also indicates that there have been changes in streamflow at the HBEF (Table 5). The 90th percentile daily streamflow threshold ranged from 5.4 to 6.3 mm across watersheds for all years evaluated, and the 75th percentile daily streamflow threshold ranged from 2.2 to 2.5 mm. In general, the number of high-flow days increased, and the number of low-flow days decreased. Increases in high-flow days were only statistically significant at W3 for the 90th ($p = 0.092$) and 75th ($p = 0.015$) percentiles, when all the years of available data were included (Table 5). The 10th percentile flow threshold ranged from 0.05 to 0.14 mm across watersheds for all years evaluated, and the 25th percentile flow threshold ranged from 0.29 to 0.42 mm. For the 25th flow percentile, the only significant trend was a decrease in the number of low-flow days at W3 ($p = 0.020$) when all the available years of data were included. For the 10th flow percentile, significant decreases were found at W3 ($p = 0.003$) and W6 ($p = 0.054$) when all the available years were included.

[29] Significant changes in the components of the hydrologic cycle (precipitation, streamflow, and ET) were detected at W3 and W6 (Figure 6). At W3, there were significant increases in precipitation (slope = +3.3 mm yr^{-1}, $p = 0.052$) and streamflow (slope = +4.5 mm yr^{-1}, $p = 0.004$) and a significant decrease in ET (slope = −1.7 mm yr^{-1}, $p = 0.054$). At W6, only trends in streamflow (slope = +3.5 mm yr^{-1}, $p = 0.082$) and ET (slope = −2.1 mm yr^{-1}, $p = 0.020$) were significant. None of the other components of the hydrologic cycle had significant time trends, although the direction of change (increasing precipitation and streamflow and decreasing ET) was the same.

3.2. Model Evaluation

[30] PnET-BGC simulations were evaluated by comparing modeled monthly streamflow with streamflow measured at W6 from WY 1964–2008 (Figure 7). Overall, the model performed well and adequately characterized streamflow during the 45 year record. In general, watershed streamflow simulations are considered satisfactory if NSME > 0.5, RSR ≤ 0.70, and PBIAS is within ±25% (Table 2) [*Moriasi et al.*, 2007]. In this study, the NSME coefficient was 0.71, indicating that there was a good fit between modeled and measured streamflow. The low RSR value (0.54) shows that the model produced little residual

Table 4. Changes in the Center of Volume Dates at W3, W6, W7, and W8[a]

Center of Volume	W3	W6	W7	W8
Annual (all years available)	−0.19 (0.180)	−0.33 (0.081)[b]	−0.32 (0.082)[b]	−0.45 (0.040)[c]
Annual (1969–2008)	−0.22 (0.363)	−0.26 (0.310)	−0.38 (0.086)[b]	−0.45 (0.040)[c]
Fall (all years available)	−0.03 (0.782)	−0.08 (0.674)	0.10 (0.537)	0.00 (0.954)
Fall (1969–2008)	−0.14 (0.568)	−0.14 (0.568)	−0.02 (0.916)	0.00 (0.954)
Winter/spring (all years available)	−0.18 (0.040)[c]	−0.17 (0.147)	−0.24 (0.030)[c]	−0.25 (0.035)[c]
Winter/spring (1969–2008)	−0.16 (0.253)	−0.12 (0.407)	−0.23 (0.065)[b]	−0.25 (0.035)[c]

[a]The KTRL slope (d yr^{-1}) and associated p values are shown for all the years available (W3, WY 1958–2008; W6, WY 1964–2008; W7, WY 1966–2008; W8, WY 1969–2008) and for a common time frame (WY 1969–2008). Fall is defined as October–December, and winter/spring is January–June.
[b]Significance $p < 0.10$.
[c]Significance $p < 0.05$.

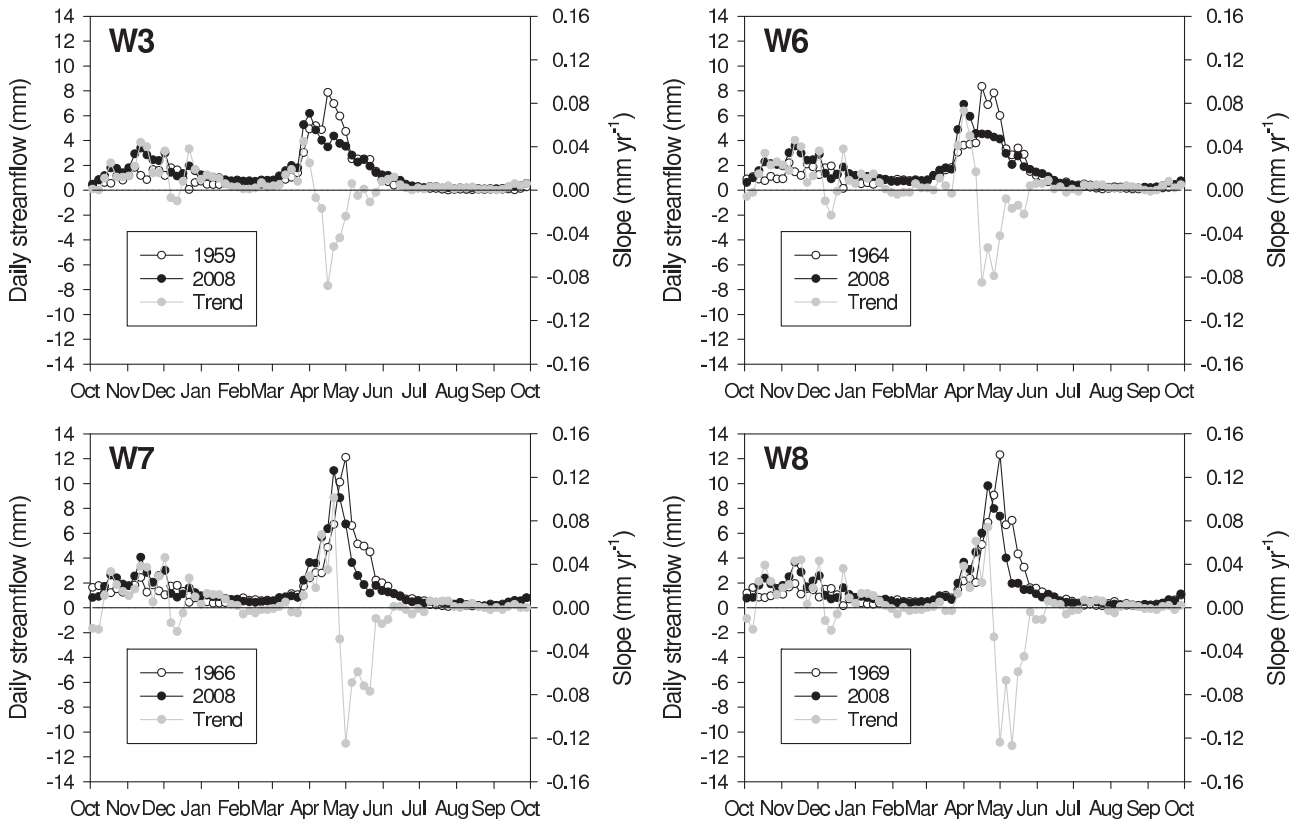

Figure 5. Changes in streamflow timing at W3, W6, W7, and W8 as indicated by sequent 5 day mean values for the initial and final years of the record calculated from the end points of the Kendall-Theil robust line. The slope is shown on the secondary *y* axis.

variation. The model also had very little bias (+1.8%) and therefore did not have a tendency over or underestimate streamflow.

3.3. Future Hydroclimatological Trends

[31] Statistically downscaled climate projections used to drive PnET-BGC showed an annual warming trend of 0.017°C–0.087°C yr^{-1}, or a total of 1.5°C–7.9°C for the 91 years from 2009–2099 (Figure 8). Air temperature increases were distributed fairly evenly over the four seasons. Annual precipitation projections also showed increases, amounting to 0.32–3.46 mm yr^{-1}, or 21–315 mm total for 2009–2099. Significant changes over time in precipitation occurred under four of the six climate change scenarios. The greatest precipitation increases over time occurred during winter, whereas there was little change to slightly decreasing precipitation amounts during summer.

[32] The most notable trend in streamflow under the four different model run types (with and without CO_2 and with and without increased precipitation) was a seasonal shift, specifically, a shift toward higher winter flows and lower spring flows (Figure 8). Summer streamflow decreased slightly, with significant slopes ranging from −0.06 to −0.11 mm yr^{-1}, with all but one significant trend occurring

Table 5. Change in the Number of Days per Year That Streamflow Exceeds High Daily Flow (75th and 90th Percentiles) and Falls Below Low-Flow (25th and 10th Percentiles) Thresholds[a]

		High-Flow Days		Low-Flow Days	
Watershed	Water Year	>90th	>75th	<25th	<10th
W3	1959–2008	+0.21 (0.092)[b]	+0.67 (0.015)[c]	−0.82 (0.020)[c]	−0.79 (0.003)[c]
	1969–2008	0.00 (0.963)	+0.33 (0.388)	−0.05 (0.916)	−0.42 (0.327)
W6	1964–2008	+0.11 (0.299)	+0.50 (0.120)	−0.36 (0.395)	−0.62 (0.054)[b]
	1969–2008	+0.05 (0.753)	+0.40 (0.263)	−0.22 (0.632)	−0.42 (0.294)
W7	1966–2008	+0.11 (0.290)	+0.27 (0.438)	−0.12 (0.769)	−0.31 (0.245)
	1969–2008	+0.05 (0.666)	+0.33 (0.435)	−0.23 (0.771)	−0.34 (0.248)
W8	1969–2008	+0.02 (0.852)	+0.43 (0.253)	−0.17 (0.789)	−0.19 (0.633)

[a]The KTRL slope (d yr^{-1}) and associated *p* values are shown for all the years available and for a common time frame (WY 1969–2008).
[b]Significance $p < 0.10$.
[c]Significance $p < 0.05$.

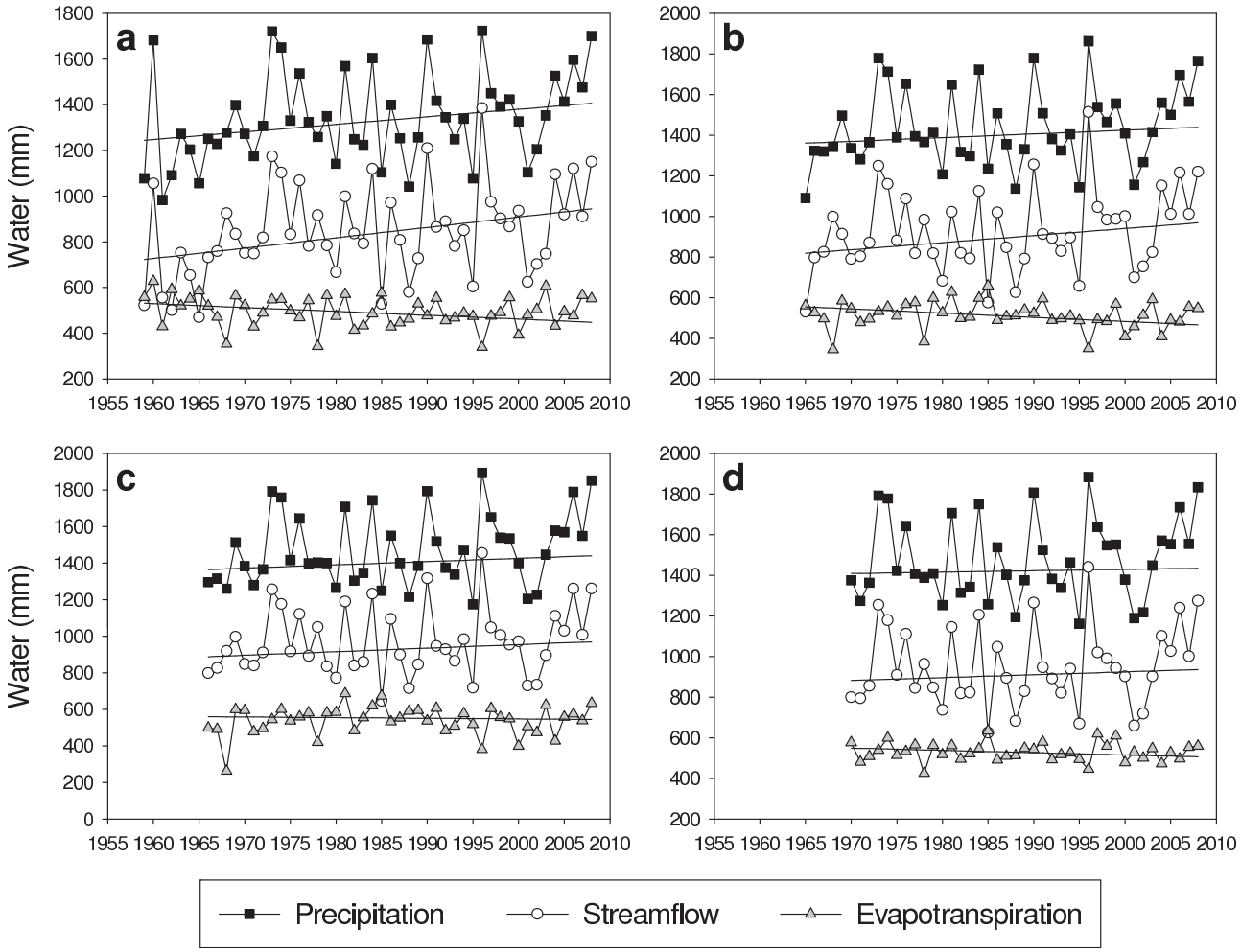

Figure 6. Long-term trends in the annual water balance at (a) W3, (b) W6, (c) W7, and (d) W8. Significant trends in precipitation (slope = +3.3 mm yr^{-1}, $p = 0.052$), streamflow (slope = +4.5 mm yr^{-1}, $p = 0.004$), and evapotranspiration (slope = −1.7 mm yr^{-1}, $p = 0.054$) were detected at W3 and in streamflow (slope = +3.5 mm yr^{-1}, $p = 0.082$) and evapotranspiration (slope = −2.1 mm yr^{-1}, $p = 0.020$) at W6.

in cases where the model was run with detrended precipitation. Fall streamflow increased significantly in two cases by 0.51 and 0.59 mm yr^{-1} when the model was run with projected increases in precipitation combined with the CO_2 effect on vegetation.

[33] Changes in total annual streamflow were relatively minor compared to changes during winter and spring. In general, when CO_2 fertilization was considered in simulations, annual streamflows increased. Significant increases ($p < 0.10$) in annual streamflow were observed under three of the six model scenarios when the CO_2 fertilization was included and under one scenario when the CO_2 effect was not included. No significant trends in streamflow were detected when the model was run with detrended precipitation.

[34] Annual precipitation, ET, and streamflow for the reference period (WY 1965–2008) compared to two future time periods (WY 2010–2054 and WY 2055–2099) indicated projected shifts in the water balance (Table 6). Precipitation increased in all cases, and the change was distributed fairly evenly between time periods. Evapotranspiration also increased, with the greatest change occurring between the reference period and WY 2010–2054. In most cases, the total increase in ET nearly offset the increase in precipitation, resulting in comparatively small changes in streamflow (−11 to + 3%).

4. Discussion

4.1. Changes in Climate

[35] Long-term measurements of air temperature and precipitation at the HBEF indicate that the climate has changed at the site, consistent with patterns of change across the broader Northeast region [*Hayhoe et al.*, 2007; *Keim et al.*, 2003, 2005; *Trombulak and Wolfson*, 2004]. Increases in air temperature and precipitation at the HBEF cannot be attributed to changes in instrumentation or measurement methodology since the same equipment and procedures have been used since the inception of the HBEF in 1955. Similarly, long-term instrument drift is not an issue since measurement devices have been calibrated regularly, and in some cases, replaced entirely.

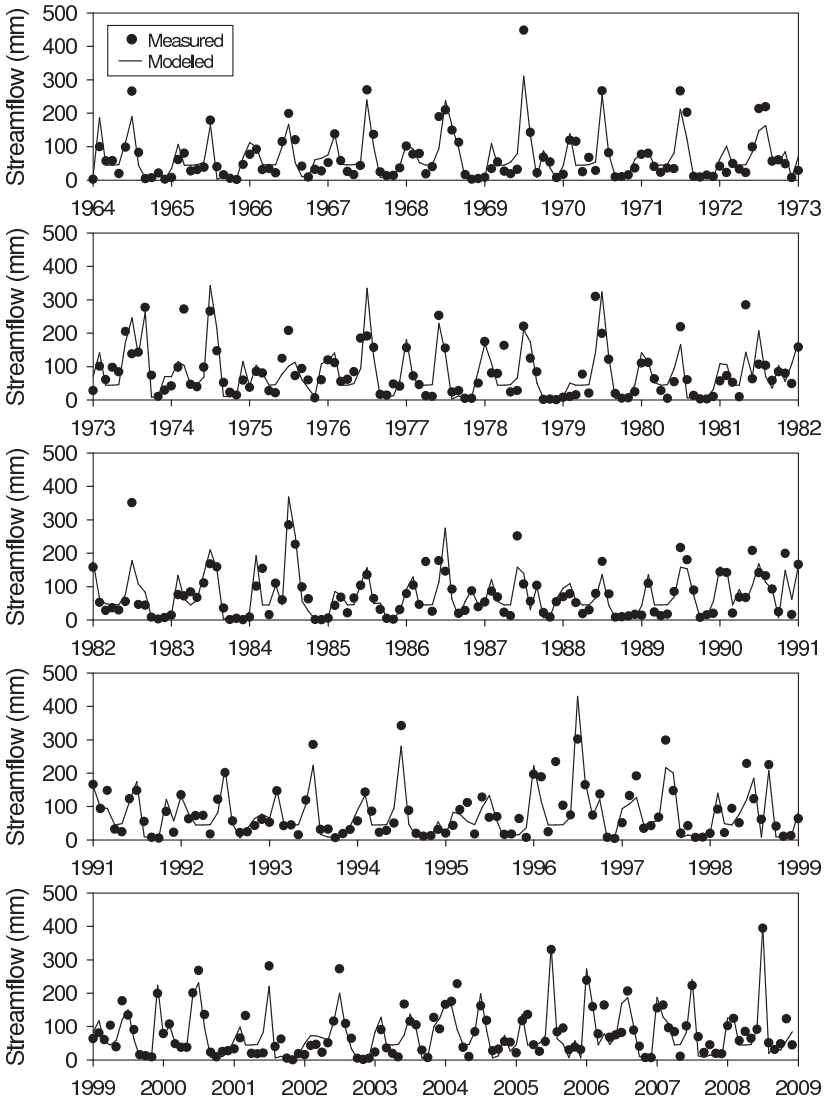

Figure 7. Comparison of streamflow measured at W6 and modeled with PnET-BGC for WY 1964–2009.

[36] Measurements of air temperature from the four weather stations with long-term records provide independent evidence that annual trends in temperature are clear and consistent across the HBEF (Figure 4). This pattern of increasing air temperature is also corroborated by longer records from other locations in the region [*Keim et al.*, 2003; *Trombulak and Wolfson*, 2004]. Projected future air temperature for all scenarios showed significant increases through the end of the century with fairly even distribution over the four seasons. Trends in air temperature under the higher GHG emission scenarios (A1FI) were greater than the measured long-term air temperature, whereas the lower GHG emission scenarios (B1) have lower and nearly identical slopes as past trends. On the basis of these results, controls on future GHG emissions could have an important influence on the trajectory of temperature change.

[37] In comparison to air temperature, long-term precipitation trends are more ambiguous. Increases in annual precipitation were measured at all sites; however, the trends were only significant at W3, which had the longest record. This trend appears to be influenced by a widespread drought that occurred across the northeastern United States in the early 1960s (Figure 6) [*Namias*, 1966]. Precipitation measurements for the other watersheds started between WY 1965 and 1970 and therefore did not capture this period of prolonged drought. Longer-term precipitation records from other locations in New Hampshire dating back to the 1930s show historical trends of decreasing precipitation to the north and increasing precipitation to the south of the HBEF [*Keim et al.*, 2005], making it difficult to determine if the 50 year trend at the HBEF is part of a longer-term regional trend. In general, the broader Northeast region has experienced increases in precipitation despite declines in some isolated areas [*Hayhoe et al.*, 2007; *Keim et al.*, 2005].

[38] Statistically downscaled climate projections for the HBEF indicate that historical increases in precipitation are expected to continue through the end of the century. At the HBEF and throughout the greater Northeast region, increases in precipitation are projected for all seasons

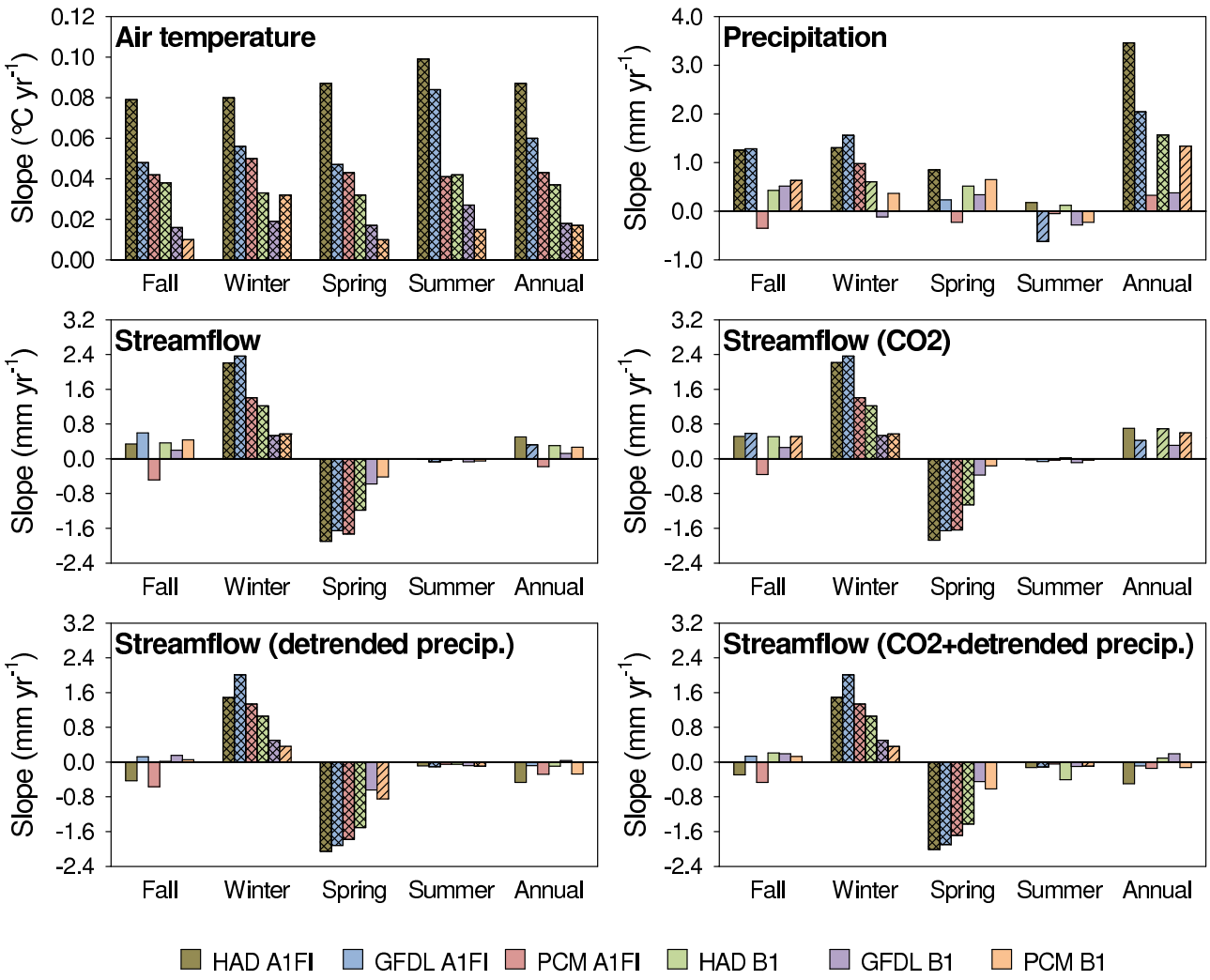

Figure 8. Seasonal and annual trends for all model scenarios, WY 2009–2099. Streamflow results are from PnET-BGC model runs with and without CO_2 fertilization effects using both projected future trends in precipitation and detrended precipitation as model input. Crosshatches indicate the 0.05 level of significance, and single hatches indicate the 0.10 level of significance.

except summer, which shows little change to slight decreases in rainfall [*Hayhoe et al.*, 2007]. Regional precipitation projections also reflect past trends. Precipitation is expected to continue to decrease in the northern part of the domain and increase to the south of the HBEF, with some spatial variability in projections arising from differences in downscaling methods [*Hayhoe et al.*, 2008].

4.2. Changes in Streamflow

[39] Past changes in climate have altered the timing and distribution of streamflow at the HBEF. The winter/spring CVD is arriving sooner, whereas there has been no significant change in the fall CVD. These seasonal patterns indicate that changes in annual trends are attributable to changes that have occurred during winter/spring. While data from the HBEF are from small headwater streams, similar trends toward earlier CVDs have been reported for larger rivers in New England [*Hodgkins et al.*, 2003]. At the HBEF, changes in streamflow timing have been accompanied by an attenuation of the snowmelt hydrograph peak (Figure 5). Significant declines in snow depth, snow water equivalent, and snow cover duration provide evidence of a diminishing snowpack at the HBEF (Table 3) [*Campbell et al.*, 2010]. Declines in snowpack water storage alter the timing of snowmelt recharge, potentially affecting streamflow during other times of the year. The most significant changes in streamflow timing were at the higher-elevation, north facing watersheds (W7 and W8) where the snowpack is deeper, lasts longer, and therefore has a greater effect on spring streamflow.

[40] The decreasing snowpack is projected to continue with time at the HBEF [*Campbell et al.*, 2010], which would be expected to influence further the seasonal distribution of streamflow. Projected model trends in the seasonal distribution of streamflow from PnET-BGC largely were consistent with past observations. Winter streamflow increased significantly under all scenarios and spring streamflows declined (Figure 8). Changes in streamflow during fall and summer were relatively minor compared to changes during winter and spring. Fall trends were

Table 6. Mean Precipitation, Evapotranspiration, and Streamflow for the Reference Period and the Change in the Mean for Two Future Time Periods and the Total Change for the Models Tested[a]

	Years	Precipitation (mm)	Evapotranspiration (mm)	Streamflow (mm)
Reference	1965–2008	1439	515	924
HAD A1FI	2010–2054	+124 (+9%)	+167 (+32%)	−43 (−5%)
	2055–2099	+171 (+11%)	+123 (+18%)	+48 (+5%)
Total Δ		+295 (+21%)	+290 (56%)	+5 (+1%)
GFDL A1FI	2010–2054	+94 (+6%)	+129 (+25%)	−36 (−4%)
	2055–2099	+92 (+6%)	+34 (+5%)	+60 (+7%)
Total Δ		+186 (+13%)	+163 (32%)	+24 (+3%)
PCM A1FI	2010–2054	+34 (+2%)	+120 (+23%)	−86 (−9%)
	2055–2099	+20 (+1%)	+32 (+5%)	−12 (−1%)
Total Δ		+54 (+4%)	+152 (29%)	−98 (−11%)
HAD B1	2010–2054	+135 (+9%)	+176 (+34%)	−42 (−5%)
	2055–2099	+60 (+4%)	+37 (+5%)	+24 (+3%)
Total Δ		+195 (+14%)	+213 (+41%)	−18 (−2%)
GFDL B1	2010–2054	+108 (+8%)	+119 (+23%)	−11 (−1%)
	2055–2099	+37 (+2%)	+7 (+1%)	+31 (+3%)
Total Δ		+145 (+10%)	+126 (+25%)	+20 (+2%)
PCM B1	2010–2054	+25 (+2%)	+128 (+25%)	−103 (−11%)
	2055–2099	+96 (+7%)	+17 (+3%)	+79 (+10%)
Total Δ		+131 (+8%)	+145 (+28%)	−24 (−3%)

[a]Values expressed as a percentage are shown in parentheses. Future data are from PnET-BGC runs (with CO_2 effect on vegetation) using the six climate change scenarios as model input. Evapotranspiration for the reference period is calculated as the difference between measured precipitation and streamflow at W6.

generally inconsistent but increased under two scenarios when CO_2 fertilization was considered (Figure 8). These scenarios had significant increases in fall precipitation that when combined with the relatively minor influence of CO_2 effects on vegetation, resulted in significantly greater streamflow. Summer streamflows declined significantly under two scenarios (GFDL A1FI and PCM B1), suggesting that summer droughts could become more prevalent; however, declines were relatively minor and were only significant under one scenario (GFDL A1FI) when precipitation was not detrended (Figure 8).

4.3. Influence of Precipitation on Streamflow

[41] Past increases in streamflow over the period of measurement (Figure 6) are due primarily to an increase in precipitation. A strong relationship exists between annual precipitation and streamflow at the four watersheds investigated (r^2 from 0.89 to 0.95), so the increase in precipitation that has occurred over the long-term record at the HBEF is reflected in stream water yield. Model runs with projected precipitation increases resulted in increased annual water yield under some scenarios, whereas model runs with detrended precipitation had negligible change in annual water yield. These results highlight the critical need to correctly characterize future precipitation for accurate streamflow forecasting.

[42] In addition to annual water yield, increases in precipitation also strongly influenced streamflow extremes, as indicated by changes in low and high flows. The number of low-flow days decreased over the measurement period, despite changes in the quantity of snowmelt runoff. These results are consistent with increases in annual minimum streamflow that have been reported in the eastern United States [*McCabe and Wolock*, 2002]. Snowmelt recharges groundwater reserves, providing water supply during base flow in summer. Earlier spring runoff could cause a longer period of low-flow recession in the summer, resulting in an increase in the number of low-flow days. *Hayhoe et al.* [2007] project a longer summer low-flow period during the 21st century, particularly under higher emission scenarios; however, historical regional data from gauged rivers provide no clear evidence of this trend [*Hodgkins et al.*, 2005]. Our results indicate that the effect of declining snowmelt recharge on streamflow is minor when compared to the effect of increasing precipitation.

[43] High flows were also strongly affected by changes in precipitation. At the HBEF the hydrograph reaches its annual maxima during spring snowmelt, so a declining snowpack could potentially decrease the number of high-flow days. Our results showed an opposite trend, characterized by an increase in the number of high-flow days. This finding stems from the fact that even though streamflow is greater on average during snowmelt, not all high-flow events occur during this period. Flood flows can happen at any time of the year at the HBEF [*Hornbeck and Kochenderfer*, 2004], and some of the greatest flows result from large frontal systems associated with hurricanes or tropical storms during fall or from extreme events that occur at other times of the year (e.g., nor'easters and thunderstorms). As with low flow, the past increase in precipitation was the dominant factor contributing to the increase in the number of high-flow days. While there may be an overall decline in the spring snowmelt peak, impacts from individual storms could increase because of more rainfall and a greater frequency and intensity of extreme precipitation events [*Easterling et al.*, 2000; *O'Gorman and Schneider*, 2009]. These changes could have important implications for flood-related issues, such as human health and safety and the integrity and design of infrastructure (e.g., roads, bridges, and culverts).

4.4. Influence of Evapotranspiration on Streamflow

[44] ET, estimated as precipitation minus runoff, has decreased over the last half century at the HBEF, yet the cause of this trend is unclear. Many potential factors influence ET, and the relationships are complex and difficult to

distinguish. The water balance calculation assumes that the storage term does not change over time, which is a reasonable assumption, given that the watersheds investigated have remained relatively undisturbed. However, it is likely that changes in watershed vegetation could influence ET rates. One might hypothesize that long-term declines in ET are due to decreases in net primary productivity. Aboveground net primary productivity (ANPP) has been calculated for various time intervals at the HBEF using allometric equations and measurements of radial tree growth [*Fahey et al.*, 2005; *Whittaker et al.*, 1974]. ANPP on W6 has been estimated as the annual increase in woody biomass plus production of annual tissues (e.g., leaves and fruits), with a correction for tree mortality. During the first 10 years of the hydrologic record (1956–1965), estimated ANPP was 420 g C m^{-2} yr^{-1} [*Whittaker et al.*, 1974]. ANNP was substantially higher from 1956–1960 (462 g C m^{-2} yr^{-1}) compared to 1961–1965 (380 g C m^{-2} yr^{-1}), which the authors attribute to low productivity associated with the prolonged drought of the early 1960s. *Fahey et al.* [2005] used the same allometric approach for estimating ANPP for 1996–1998 and found that it was 354 g C m^{-2} yr^{-1}, a 23% decline since the beginning of the hydrologic record. The reason for the decline in ANPP at the HBEF is not fully understood but is thought to reflect a combination of age-related growth declines and accelerated tree mortality. Recent declines in aboveground biomass have been attributed to increased mortality of the dominant species (sugar maple, American beech, and yellow birch [*Campbell et al.*, 2007; *Siccama et al.*, 2007]). Beech bark disease, which typically kills older American beech trees, has contributed to recent biomass declines in larger size classes. Some evidence indicates that observed declines in sugar maple biomass could be due to declining site quality associated with depletion of soil available calcium [*Juice et al.*, 2006; *Likens et al.*, 1998]. Yellow birch has also declined in recent years. Widespread birch decline has been reported previously in the region and has been attributed, at least in part, to climatic events such as drought and soil frost [*Bourque et al.*, 2005]. In addition to decreases in the accumulation rate of tree biomass, long-term declines in ET could also be due to decreases in biomass of other classes of vegetation (e.g., seedlings and herbs). It is also possible that shifts in the composition of vegetation to species with lower transpiration rates could have contributed to observed declines in ET.

[45] Declines in ET could also be the result of atmospheric CO_2 concentration effects on plant gas exchange. As atmospheric CO_2 concentration increases, stomatal conductance decreases [*Franks and Beerling*, 2009]. This process can limit transpirational water loss, potentially causing increased streamflow [*Gedney et al.*, 2006], although effects on streamflow are not well established and remain contentious [*Huntington*, 2008; *Peel and McMahon*, 2006]. Climate-related factors could also limit ET, such as increases in specific humidity. Widespread increases in surface humidity and cloudiness, consistent with increasing trends in precipitation, have been detected over the last century and are attributed to increasing temperatures [*Henderson-Sellers*, 1992; *Willett et al.*, 2007].

[46] Despite slight historical declines in ET, PnET-BGC model simulations indicated that future ET will increase over the 21st century. These increases in ET are due mostly to increases in transpiration, which greatly exceed evaporative losses at the HBEF [*Campbell et al.*, 2009]. Previous model results from the HBEF indicate that NPP increased over the 21st century, causing sustained increases in transpiration [*Campbell et al.*, 2009]. The warmer and wetter future climate increased decomposition rates of soil organic matter, which is coupled with nutrient mineralization in the model. The increased nutrient availability, combined with increased temperature and precipitation, resulted in a longer and more productive growing season. Interestingly, some declines in transpiration were observed during midsummer because of drought stress associated with declining soil moisture content and higher vapor pressure deficits under future climate change scenarios [*Campbell et al.*, 2009]. In the model, midsummer drought stress reduced foliage production; however, wood growth continued to increase because of the longer growing season and higher canopy photosynthetic rates during the nonstressed time periods [*Campbell et al.*, 2009].

[47] Because of the nonlinear response of photosynthesis to CO_2, the increasing trend in ET diminished over time, with greater increases during the first half of the century compared to the latter half. Inclusion of the CO_2 effect on vegetation in the model caused slight increases in streamflow relative to model runs when CO_2 fertilization was not considered because increasing atmospheric CO_2 concentrations decrease stomatal conductance (Figure 6). Increases in atmospheric CO_2 reduced the amount of transpiration in the model, thereby minimizing water loss to the atmosphere and increasing streamflow.

[48] Changes in streamflow at the HBEF were relatively modest when compared to simulations for other forested sites in the region [*Ollinger et al.*, 2008]. Streamflow did not change much at the HBEF because the higher ET was offset by precipitation increases (Table 6). In other forest ecosystems, particularly those dominated by conifers which are more susceptible to temperature stress, NPP may begin to decline, resulting in declines in ET and increases in streamflow [*Ollinger et al.*, 2008].

5. Conclusions

[49] Determining the effect of climate change on streamflow involves understanding complex interactions among atmospheric, terrestrial, and aquatic processes. In this study we used long-term measurements from the HBEF to evaluate trends in streamflow. We also modeled streamflow through the end of the 21st century using the forest ecosystem model PnET-BGC, driven by future climate change scenarios from downscaled AOGCM output. Results from long-term streamflow measurements indicated that the snowmelt peak is occurring earlier now as compared to the beginning of the record and has decreased in magnitude, a trend that is expected to continue in the future. These changes are attributed to measured and modeled snowpack declines and earlier snowmelt. Significant increases in annual water yield have been observed over the long-term record at the HBEF, largely in response to increases in precipitation. Interestingly, slight, but significant, declines in ET have also been observed, yet the explanation for this trend is unclear. Future research should focus on identifying the cause of this decline so that the dominant controls

can be adequately represented in process-based models. Contrary to past trends, results from future PnET-BGC simulations showed that ET is projected to increase largely because of effects of a warmer, wetter climate on forest growth. A major uncertainty in these forecasts is the impact of increasing CO_2 on forest vegetation. Even though experimental manipulations have shown that atmospheric CO_2 enhances NPP and, hence, ET, it is unclear whether this growth can be sustained as vegetation acclimates to higher atmospheric CO_2 concentrations. Uncertainty remains as to whether increases in atmospheric CO_2 concentrations suppress transpiration over the long term and the extent to which this process affects streamflow. In addition to continued refinement of the processes depicted in models, there is also a critical need to continue to refine future climate projections used as input to ecosystem models. Decreasing the uncertainty of future precipitation is particularly important since it has a large impact on streamflow, with marked effects on high and low flows. A more thorough understanding of climate change impacts on streamflow will enable us to better prepare for and adapt to changes that may occur, which is particularly important in the northeastern United States because of the high population density and strong reliance on stream generation from higher elevation watersheds.

[50] **Acknowledgments.** The authors would like to thank Thomas Huntington, Chelcy Ford, and three anonymous referees for providing helpful comments that improved this manuscript. Amey Bailey compiled the long-term hydrometeorological data collected at the HBEF. Funding for this study was provided by the Environmental Protection Agency and the USDA Northeastern States Research Cooperative. This manuscript is a contribution of the Hubbard Brook Ecosystem Study. Hubbard Brook is part of the Long-Term Ecological Research (LTER) network, which is supported by the National Science Foundation. The Hubbard Brook Experimental Forest is operated and maintained by the USDA Forest Service, Northern Research Station, Newtown Square, Pennsylvania.

References

Aber, J. D., and C. A. Federer (1992), A generalized, lumped-parameter model of photosynthesis, evapotranspiration and net primary production in temperate and boreal forest ecosystems, *Oecologia*, *92*, 463–474.

Aber, J. D., and R. Freuder (2000), Variation among solar radiation data sets for the eastern US and its effects on predictions of forest production and water yield, *Clim. Res.*, *15*, 33–43.

Bailey, A. S., J. W. Hornbeck, J. C. Campbell, and C. Eagar (2003), Hydrometeorological database for Hubbard Brook Experimental Forest: 1955–2000, *Gen. Tech. Rep. NE-305*, 36 pp., Northeast. Res. Stn., For. Serv., U.S. Dep. of Agric., Newtown Square, Pa.

Barnett, T. P., J. C. Adam, and D. P. Lettenmaier (2005), Potential impacts of a warming climate on water availability in snow-dominated regions, *Nature*, *438*, 303–309.

Bourque, C. P.-A., R. M. Cox, D. J. Allen, P. A. Arp, and F.-R. Meng (2005), Spatial extent of winter thaw events in eastern North America: Historical weather records in relation to yellow birch decline, *Global Change Biol.*, *11*, 1477–1492.

Burakowski, E. A., C. P. Wake, B. Braswell, and D. P. Brown (2008), Trends in wintertime climate in the northeastern United States: 1965–2005, *J. Geophys. Res.*, *113*, D20114, doi:10.1029/2008JD009870.

Campbell, J. L., et al. (2007), Long-term trends from ecosystem research at the Hubbard Brook Experimental Forest, *Gen. Tech. Rep. NRS-17*, 41 pp., Northeast. Res. Stn., For. Serv., U.S. Dep. of Agric., Newtown Square, Pa.

Campbell, J. L., et al. (2009), Consequences of climate change for biogeochemical cycling in forests of northeastern North America, *Can. J. For. Res.*, *39*, 264–284.

Campbell, J. L., S. V. Ollinger, G. N. Flerchinger, H. Wicklein, K. Hayhoe, and A. S. Bailey (2010), Past and projected future changes in snowpack and soil frost at the Hubbard Brook Experimental Forest, New Hampshire, USA, *Hydrol. Processes*, *24*, 2465–2480.

Cayan, D. R., S. A. Kammerdiener, M. D. Dettinger, J. M. Caprio, and D. H. Peterson (2001), Changes in the onset of spring in the western United States, *Bull. Am. Meteorol. Soc.*, *82*, 399–415.

Chen, L., and C. T. Driscoll (2005a), Regional application of an integrated biogeochemical model to northern New England and Maine, *Ecol. Appl.*, *15*, 1783–1797.

Chen, L., and C. T. Driscoll (2005b), Regional assessment of the response of the acid-base status of lake watersheds in the Adirondack region of New York to changes in atmospheric deposition using PnET-BGC, *Environ. Sci. Technol.*, *39*, 787–794.

Christensen, N. C., A. W. Wood, N. Voisin, D. P. Lettenmaier, and R. N. Palmer (2004), The effects of climate change on the hydrology and water resources of the Colorado River Basin, *Clim. Change*, *62*, 337–363.

Court, A. (1962), Measures of streamflow timing, *J. Geophys. Res.*, *67*, 4335–4339.

Davies, T. D., and S. J. Vavrus (1991), Climatic change and seasonal snowcovers: A review of the factors regulating the chemical evolution of snowcover and a predictive case study for north-eastern North America, in *NATO Advanced Research Workshop on Processes of Chemical Change in Snowpacks, NATO ASI Series, Ser. G*, vol. 28, edited by T. D. Davies, M. Tranter, and H. G. Jones, pp. 421–456, Springer, Berlin.

Delworth, T. L., et al. (2006), GFDL's CM2 global coupled climate models. Part 1: Formulation and simulation characteristics, *J. Clim.*, *19*, 643–674.

Déry, S. J., K. Stahl, R. D. Moore, P. H. Whitfield, B. Menounos, and J. E. Burford (2009), Detection of runoff timing changes in pluvial, nival, and glacial rivers of western Canada, *Water Resour. Res.*, *45*, W06701, doi:10.1029/2009WR008244.

Dettinger, M. D., and D. R. Cayan (1995), Large-scale atmospheric forcing of recent trends toward early snowmelt runoff in California, *J. Clim.*, *8*, 606–623.

Dore, M. H. I. (2005), Climate change and changes in global precipitation patterns: What do we know?, *Environ. Int.*, *31*, 1167–1181.

Easterling, D. R., G. A. Meehl, C. Parmesan, S. A. Changnon, T. R. Karl, and L. O. Mearns (2000), Climate extremes: Observations, modeling, and impacts, *Science*, *289*, 2068–2074.

Fahey, T. J., et al. (2005), The biogeochemistry of carbon at Hubbard Brook, *Biogeochemistry*, *75*, 109–179.

Franks, P. J., and D. J. Beerling (2009), Maximum leaf conductance driven by CO_2 effects on stomatal size and density over geologic time, *Proc. Natl. Acad. Sci. U. S. A.*, *106*, 10,343–10,347.

Gbondo-Tugbawa, S. S., and C. T. Driscoll (2003), Factors controlling long-term changes in soil pools of exchangeable basic cations and stream acid neutralizing capacity in a northern hardwood forest ecosystem, *Biogeochemistry*, *63*, 161–185.

Gbondo-Tugbawa, S. S., C. T. Driscoll, J. D. Aber, and G. E. Likens (2001), Validation of a new integrated biogeochemical model (PnET-BGC) at a northern hardwood forest ecosystem, *Water Resour. Res.*, *37*, 1057–1070.

Gbondo-Tugbawa, S. S., C. T. Driscoll, M. J. Mitchell, J. D. Aber, and G. E. Likens (2002), A model to simulate the response of a northern hardwood forest ecosystem to changes in S deposition, *Ecol. Appl.*, *12*, 8–23.

Gedney, N., P. M. Cox, R. A. Betts, O. Boucher, C. Huntingford, and P. A. Stott (2006), Detection of a direct carbon dioxide effect in continental river runoff records, *Nature*, *439*, 835–838.

Hartley, S., and S. L. Dingman (1993), Effects of climatic variability on winter-spring runoff in New England river basins, *Phys. Geogr.*, *14*, 379–393.

Hayhoe, K., et al. (2007), Past and future changes in climate and hydrological indicators in the US Northeast, *Clim. Dyn.*, *28*, 381–407.

Hayhoe, K., C. Wake, B. Anderson, X. Liang, E. Maurer, J. Zhu, J. Bradbury, A. DeGaetano, A. Stoner, and D. Wuebbles (2008), Regional climate change projections for the northeast USA, *Mitigation Adapt. Strategies Global Change*, *13*, 425–436.

Helsel, D. R., and R. M. Hirsch (1992), *Statistical Methods in Water Resources*, Elsevier Sci., Amsterdam.

Henderson-Sellers, A. (1992), Continental cloudiness changes this century, *GeoJournal*, *27*, 255–262.

Hidalgo, H. G., et al. (2009), Detection and attribution of streamflow timing changes to climate change in the western United States, *J. Clim.*, *22*, 3838–3855.

Hirsch, R. M., and J. R. Slack (1984), Non-parametric trend test for seasonal data with serial dependence, *Water Resour. Res.*, *20*, 727–732.

Hirsch, R. M., J. R. Slack, and R. A. Smith (1982), Techniques of trend analysis for monthly water quality data, *Water Resour. Res.*, *18*, 107–121.

Hodgkins, G. A., and R. W. Dudley (2005), Changes in the magnitude of annual and monthly streamflows in New England, 1902–2002, *U.S. Geol. Surv. Sci. Invest. Rep., 2005-5135*.

Hodgkins, G. A., and R. W. Dudley (2006), Changes in late-winter snowpack depth, water equivalent, and density in Maine, 1926–2004, *Hydrol. Processes*, *20*, 741–751.

Hodgkins, G. A., R. W. Dudley, and T. G. Huntington (2003), Changes in the timing of high river flows in New England over the 20th century, *J. Hydrol.*, *278*, 244–252.

Hodgkins, G. A., R. W. Dudley, and T. G. Huntington (2005), Summer low flows in New England during the 20th century, *J. Am. Water Resour. Assoc.*, *41*, 403–412.

Hornbeck, J. W., and J. N. Kochenderfer (2004), A century of lessons about water resources in northeastern forests, in *A Century of Forest and Wildland Watershed Lessons*, edited by G. G. Ice and J. D. Stednick, pp. 19–31, Soc. of Am. For., Bethesda, Md.

Huntington, T. G. (2003), Climate warming could reduce runoff significantly in New England, USA, *Agric. For. Meteorol.*, *117*, 193–201.

Huntington, T. G. (2008), CO_2-induced suppression of transpiration cannot explain increasing runoff, *Hydrol. Processes*, *22*, 311–314.

Huntington, T. G., G. A. Hodgkins, B. D. Keim, and R. W. Dudley (2004), Changes in the proportion of precipitation occurring as snow in New England (1949–2000), *J. Clim.*, *17*, 2626–2636.

Huntington, T. G., A. D. Richardson, K. J. McGuire, and K. Hayhoe (2009), Climate and hydrological changes in the northeastern United States: Recent trends and implications for forested and aquatic ecosystems, *Can. J. For. Res.*, *39*, 199–212.

Intergovernmental Panel on Climate Change (IPCC) (2007), *Climate Change 2007: The Physical Science Basis. Contribution of Working Group I to the Fourth Assessment Report of the Intergovernmental Panel on Climate Change*, edited by S. Solomon et al., Cambridge Univ. Press, New York.

Iverson, L. R., and A. M. Prasad (1998), Predicting abundance of 80 tree species following climate change in the eastern United States, *Ecol. Monogr.*, *68*, 465–485.

Iverson, L. R., M. W. Schwartz, and A. M. Prasad (2004), How fast and far might tree species migrate under climate change in the eastern United States?, *Global Ecol. Biogeogr.*, *13*, 209–219.

Iverson, L. R., A. M. Prasad, S. N. Matthews, and M. Peters (2008), Estimating potential habitat for 134 eastern US tree species under six climate scenarios, *For. Ecol. Manage.*, *254*, 390–406.

Juice, S. M., T. J. Fahey, T. G. Siccama, C. T. Driscoll, E. G. Denny, C. Eagar, N. L. Cleavitt, M. R., and A. D. Richardson (2006), Response of sugar maple to calcium addition to northern hardwood forest at Hubbard Brook, NH, *Ecology*, *87*, 1267–1280.

Keim, B. D., A. M. Wilson, C. P. Wake, and T. G. Huntington (2003), Are there spurious temperature trends in the United States Climate Division database?, *Geophys. Res. Lett.*, *30*(7), 1404, doi:10.1029/2002GL016295.

Keim, B. D., M. R. Fischer, and A. M. Wilson (2005), Are there spurious precipitation trends in the United States Climate Division database?, *Geophys. Res. Lett.*, *32*, L04702, doi:10.1029/2004GL021985.

Kendall, M. (1938), A new measure of rank correlation, *Biometrika*, *30*, 81–93.

Likens, G. E., and F. H. Bormann (1995), *Biogeochemistry of a Forested Ecosystem*, Springer, New York.

Likens, G. E., et al. (1998), The biogeochemistry of calcium at Hubbard Brook, *Biogeochemistry*, *41*, 89–173.

McCabe, G. J., and D. M. Wolock (2002), A step increase in streamflow in the conterminous United States, *Geophys. Res. Lett.*, *29*(24), 2185, doi:10.1029/2002GL015999.

Milly, P. C. D., K. A. Dunne, and A. V. Vecchia (2005), Global pattern of trends in streamflow and water availability in a changing climate, *Nature*, *438*, 347–350.

Moriasi, D. N., J. G. Arnold, M. W. Van Liew, R. L. Bingner, R. D. Harmel, and T. L. Veith (2007), Model evaluation guidelines for systematic quantification of accuracy in watershed simulations, *Trans. ASABE*, *50*, 885–900.

Nakicenovic, N., et al. (2000), *Special Report on Emissions Scenarios. A Special Report of Working Group III of the Intergovernmental Panel on Climate Change*, Cambridge Univ. Press, Cambridge, U. K.

Namias, J. (1966), Nature and possible causes of the northeastern United States drought during 1962–65, *Mon. Weather Rev.*, *94*, 543–554.

Nash, J. E., and J. V. Sutcliffe (1970), River flow forecasting through conceptual models, part I—A discussion of principles, *J. Hydrol.*, *10*, 282–290.

O'Gorman, P. A., and T. Schneider (2009), The physical basis for increases in precipitation extremes in simulations of 21st-century climate change, *Proc. Natl. Acad. Sci. U. S. A.*, *106*, 14,773–14,777.

Ollinger, S. V., C. L. Goodale, K. Hayhoe, and J. P. Jenkins (2008), Potential effects of climate change and rising CO_2 on ecosystem processes in northeastern U.S. forests, *Mitigation Adapt. Strategies Global Change*, *13*, 467–485.

Peel, M. C., and T. A. McMahon (2006), Continental runoff: A quality-controlled global runoff data set, *Nature*, *444*, E14.

Pope, V. D., M. L. Gallani, P. R. Rowntree, and R. A. Stratton (2000), The impact of new physical parametrizations in the Hadley Centre climate model—HadAM3, *Clim. Dyn.*, *16*, 123–146.

Regonda, S. K., B. Rajagopalan, M. Clark, and J. Pitlick (2005), Seasonal cycle shifts in hydroclimatology over the western United States, *J. Clim.*, *18*, 372–384.

Reinhart, K. G., and R. S. Pierce (1964), Stream-gaging stations for research on small watersheds, *Agric. Handb.*, *268*, 37 pp.

Schwarz, P. A., T. J. Fahey, and C. E. McCulloch (2003), Factors controlling spatial variation of tree species abundance in a forested landscape, *Ecology*, *84*, 1862–1878.

Sen, P. K. (1968), Estimates of the regression coefficient based on Kendall's tau, *J. Am. Stat. Assoc.*, *63*, 1379–1389.

Siccama, T. G., T. J. Fahey, C. E. Johnson, T. W. Sherry, E. G. Denny, E. B. Girdler, G. E. Likens, and P. A. Schwarz (2007), Population and biomass dynamics of trees in a northern hardwood forest at Hubbard Brook, *Can. J. For. Res.*, *37*, 737–749.

Stewart, I. T., D. R. Cayan, and M. D. Dettinger (2005), Changes toward earlier streamflow timing across western North America, *J. Clim.*, *18*, 1136–1155.

Swank, W. T., and J. E. Douglass (1974), Streamflow greatly reduced by converting deciduous hardwood stands to pine, *Science*, *185*, 857–859.

Trombulak, S. C., and R. Wolfson (2004), Twentieth-century climate change in New England and New York, USA, *Geophys. Res. Lett.*, *31*, L19202, doi:10.1029/2004GL020574.

Verry, E. S. (2003), Estimating ground water yield in small research basins, *Ground Water*, *41*, 1001–1004.

Washington, W. M., et al. (2000), Parallel climate model (PCM) control and transient simulations, *Clim. Dyn.*, *16*, 755–774.

Whittaker, R. H., F. H. Bormann, G. E. Likens, and T. G. Siccama (1974), The Hubbard Brook Ecosystem Study: Forest biomass and production, *Ecol. Monogr.*, *44*, 233–254.

Willett, K. M., N. P. Gillett, P. D. Jones, and P. W. Thorne (2007), Attribution of observed surface humidity changes to human influence, *Nature*, *449*, 710–712.

Wood, A. W., E. P. Maurer, A. Kumar, and D. Lettenmaier (2002), Long-range experimental hydrologic forecasting for the eastern United States, *J. Geophys. Res.*, *107*(D20), 4429, doi:10.1029/2001JD000659.

Wood, A., L. R. Leung, V. Sridhar, and D. Lettenmaier (2004), Hydrologic implications of dynamical and statistical approaches to downscaling climate model surface temperature and precipitation fields, *Clim. Change*, *62*, 189–216.

J. L. Campbell, Northern Research Station, U.S. Forest Service, Durham, NH 03081, USA. (jlcampbell@fs.fed.us)

C. T. Driscoll and A. Pourmokhtarian, Department of Civil and Environmental Engineering, Syracuse University, Syracuse, NY 13244, USA.

K. Hayhoe, Department of Geosciences, Texas Tech University, Lubbock, TX 79409, USA.